Presented at the 21st European Photovoltaic Solar Energy Conference and Exhibition,
4-8 September 2006, Dresden, Germany

ALMOST 1% ABSOLUTE EFFICIENCY INCREASE IN MC-SI SOLAR CELL MANUFACTURING WITH SIMPLE ADJUSTMENTS TO THE PROCESSING SEQUENCE

C.J.J. Tool[1], M. Koppes[1], M. Fleuster[2], B.H.M. van Straaten[2], A.W. Weeber[1]
[1]ECN Solar Energy, PO Box 1, NL-1755 ZG Petten, The Netherlands
Tel: +31 224 564135, fax: +31 224 568214, email: tool@ecn.nl
[2] Solland Solar Energy BV, Bohr 10, 6422 RL Heerlen, The Netherlands

ABSTRACT: Due to the use of thinner and larger wafers, in-line belt diffusion becomes more commonly used in new production lines. In this paper two possible adjustments to the processing sequences with an in-line belt diffusion are discussed. Double-sided diffusion (applying phosphorous on both sides of the wafer) leads to a better gettering and a maximum absolute efficiency increase of 0.8%. The average absolute efficiency increase for double-sided diffusion is 0.5%. A simple surface cleaning before SiN_x:H ARC deposition results in better surface passivation and an additional absolute efficiency gain of 0.3%. Both the experimental results and PC-1D modeling confirms that these efficiency gains are indeed independent and can be added, so an overall efficiency gain of nearly 1% absolute can be obtained. Besides the efficiency gain, double-sided diffusion also results in a narrowing of the efficiency distribution.
Keywords: diffusion, gettering, cleaning

1 INTRODUCTION

The main focus in reducing the €/W_p cost of photovoltaics is by the use of thinner and larger wafers. However, processing these wafers in state of the art high-efficiency processes involve batch systems where wafers are handled to place them vertically, such as for $POCl_3$ diffusion. This handling increases the risk of yield losses as wafers become thinner and larger.

Belt diffusion is often thought of as an unclean process which could limit the obtainable efficiencies. We have already shown by FZ lifetime measurements that with belt furnace diffusion material quality can be preserved and average efficiencies on mc-Si of 16.5% can be realised [1]. Also we obtained efficiencies up to 17% on multi crystalline material with this in-line belt diffusion [1,2,3].

It is well known that phosphorous gettering is important in multi crystalline cell processing to improve the material quality of the wafers. This gettering acts by the diffusion of impurities from the bulk of the wafer to the surface regions. In production lines which use in-line diffusion in a belt furnace, the phosphorous source is normally applied only on one side of the wafer. This means that all impurities have to diffuse to that side. By applying phosphorous to both sides of the wafer, gettering will become more effective.

To obtain good surface passivation on test samples thorough cleanings like RCA are used. To improve the surface passivation with SiN_x:H in solar cells processing ECN applies a cleaning step after standard glass removal with HF. This ECN-clean consists of simple wet bench treatment of the cells after glass removal but before SiN_x:H deposition.

The purpose of the work presented in this paper is to show that 2 simple adjustments to an industrial in-line processing sequence can lead to a significant cell efficiency increase.

2 EXPERIMENTAL

156 cm^2 mc-Si wafers with a thickness of 330 µm were processed using an industrial type in-line process sequence. This process is based on belt diffusion, screen printing and firing-through SiN_x:H.

We used an industrial applicable acidic etch recipe to combine texturization and saw damage removal in one single process step. Depending on the group either a single-sided emitter or a double-sided emitter was realized by applying the phosphorous source on either one side or both sides of the wafer. Diffusion was carried out using industrial applicable throughputs using an IR heated belt furnace. The wafers were put directly on the metal belt with the emitter side facing up. This resulted in a 65Ω/sq emitter. After diffusion the phosphorous glass was removed using HF. Some groups were given an additional cleaning; the so called ECN-clean. This clean consists of a simple wet cleaning followed by rinsing and drying. A SiN_x:H anti reflection coating was applied using a Remote MicroWave PECVD. After screen printing of an Ag H-pattern on the front side and a full Al rear side, the metallization was co-fired in an IR heated belt furnace. All the groups were fired at the same firing condition (see Table 1). Neighboring wafers were used over the groups. The experimental matrix is given in Table 2.

Table 1: Simple in-line solar cell pricessing sequence on 156 cm^2 mc-Si wafers.

Industrial in-line solar cell processing sequence
1. Industrial isotexturing (recipe T1 in [1]) for simultaneous saw damage removal and surface texturing
2. Single-sided or double-sided spin-on phosphorous source[a] followed by infrared heated belt furnace emitter diffusion during 8 minutes at peak temperature[b] to create a 65 Ω/sq emitter
3. Phosphorous glass removal using HF optionally followed by an additional wet clean (ECN-clean)
4. $SiNH_x$:H deposition with a Remote MicroWave PECVD system
5. Screen printing of the Ag front side metallisation and full Al rear side metallisation
6. Simultaneous firing of the front and rear side metallisation and Al Back Surface Field (BSF) formation in an infrared heated belt furnace
7. Edge isolation

[a] Because spin coating is often regarded as a non-in-line, non-industrial technique, ECN together with Despatch have developed an in-line spray system to apply the phosphorous source capable of both single sided and double sided deposition. However, this system was not yet available when these experiments were conducted.

First recent result of the spraying are given in section 3.4

[b]: this is a shorter diffusion time than in our standard baseline process [4]

The current voltage measurements were performed using a class A solar simulator at ECN with 6 current probes per busbar. The measurements were performed according to the ASTM-E948 norm [5]. Spectral Response and reflection measurements were conducted to calculate the Internal Quantum Efficiency (IQE) of selected cells. The data are statistically analyzed using the computer program Statgraphics 5[+] [6]. PC-1D5.5 [7] was used for modeling to understand the observed trends.

Table 2: Experimental matrix

group	diffusion	cleaning
1	single sided	non
2	single sided	ECN-clean
3	double sided	non
4	double sided	ECN-clean

3 RESULTS AND DISCUSSION

The average values of the solar cell characteristics are given in Table 3. The efficiency gain for both process modifications results from an increase in both J_{sc} and V_{oc}. The fill factor (FF) is not significantly influenced by the changes in the processing. For both modifications, the increase in J_{sc} is more pronounced than the increase in V_{oc}.

Table 3: Average value solar cell characteristics; error margins given are the standard deviations. Because the least significant differences (LSD) were comparable within the groups the LSD at 95% confidence limit is given in for each parameter in the last row.

group	J_{sc} (mA/cm^2)	V_{oc} (mV)	FF (%)	η (%)
1: single, no clean	31.8±0.6	595±5	76.9±0.7	14.5±0.4
2: single, ECN-clean	32.4±0.6	599±4	76.3±0.5	14.8±0.4
3: double, no clean	32.7±0.3	601±1	76.6±0.4	15.0±0.2
4: double, ECN-clean	33.0±0.3	604±1	76.7±0.5	15.3±0.2
LSD-interval	0.05	0.005	0.1	0.04

3.1 Double sided diffusion

The most obvious explanation for the efficiency gain obtained with the double-sided diffusion results from better gettering. We create two gettering sinks which on average halves the diffusion distance for the impurities (Figure 1).

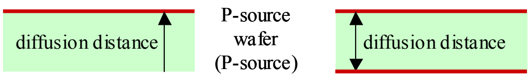

Figure 1: Impurity diffusion distance halves with double sided diffusion.

Because the effect is based on impurity gettering, it is assumed that wafers with more impurities, and thus lower cell efficiency, will show a larger efficiency gain compared to wafers with lesser impurities. This is confirmed experimentally as shown in Figure 2. This figure shows the absolute efficiency increase due to the double-sided emitter as a function of the efficiency realized with a single-sided emitter. For the cells with the lowest efficiency the increase in efficiency is up to 1% absolute, whereas for the best cells no efficiency increase occurs. This leads to a narrowing of the efficiency distribution from about 1.5% absolute to less than 0.7% absolute (Figure 4). This narrowing in efficiency distribution results from both a narrowing in the distribution of J_{sc} and V_{oc} as can be seen by the standard deviation given in Table 3. The standard deviation in J_{sc} is about halved for the double sided group compared to the single sided diffused group, while the standard deviation for V_{oc} is even more dramatically decreased. The standard deviation in FF is comparable for the two cases, indicating that the narrowing of the efficiency distribution does not result from fill factor, but indeed from a decrease in the current and voltage range obtained.

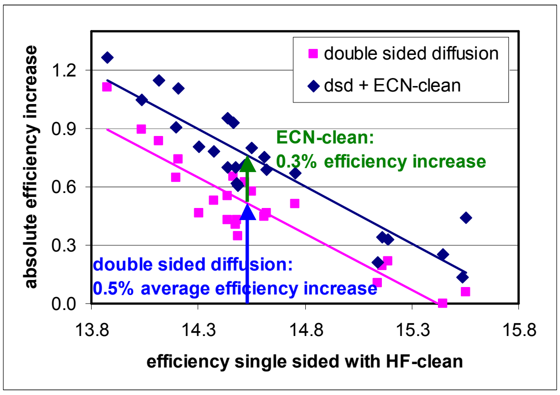

Figure 2: Absolute efficiency gain of double sided diffusion (pink) and double sided diffusion + ECN-clean (purple) compared to single sided diffusion with no additional clean. Lines drawn are least square fits to the experimental data.

The IQE measurements confirm that the red response is increased by the double diffusion, confirming that the efficiency gain results from an improvement of the bulk. Also it is found that the increase in red response depends on the efficiency obtained with a single sided diffusion. Figure 3 shows that the ratio of the red response for the double-sided diffused group over the single sided diffused group for cells with different efficiency. The dependence of the increased red response on the efficiency is clear from this plot.

These results are in agreement with the results of Goris et al [8] who investigated the influence of double sided gettering on wafer position in the ingot.

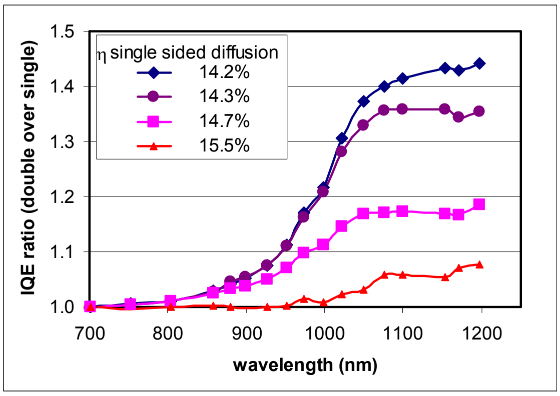

Figure 3: IQE ratio of double sided diffusion over single sided diffusion. The increase in red response is dependent on the efficiency obtained with the single sided diffusion.

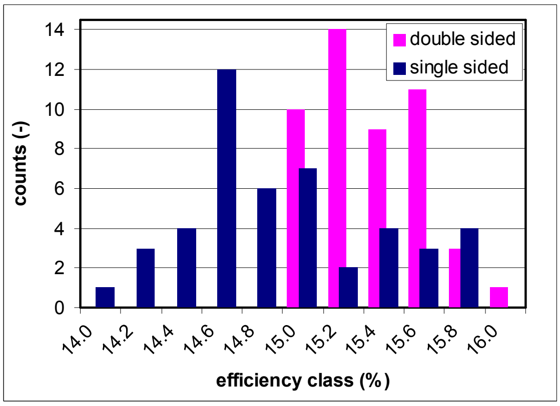

Figure 4: Efficiency distribution for both the single sided and the double sided siffused group.

3.2 Influence ECN clean

Figure 5 shows the ratio of the IQE for the ECN-cleaned group over the non-cleaned group. Clearly, the blue response of the cells increases due to the ECN-clean. Also, the increase for both the single sided diffused group and the double sided diffused group is identical.

In Figure 2 also the absolute efficiency increase due to the combined effect of the ECN-clean and the double sided diffusion is shown as a function of the efficiency obtained with single sided diffusion and only HF-clean. The gain due to the ECN-clean is the difference between the pink line (double sided diffusion + HF-clean) and the purple line (double sided diffusion + ECN-clean). The two lines have the same slope. This means that the gain due to the ECN-clean is independent of the initial efficiency and thus indicates that the obtained gains for the double-sided diffusion and the ECN-clean are independent of each other. This is also in agreement with the IQE measurements; the gain due to the ECN-clean results from an increased blue response; the gain due to the double-sided diffusion results from an increase in the red response.

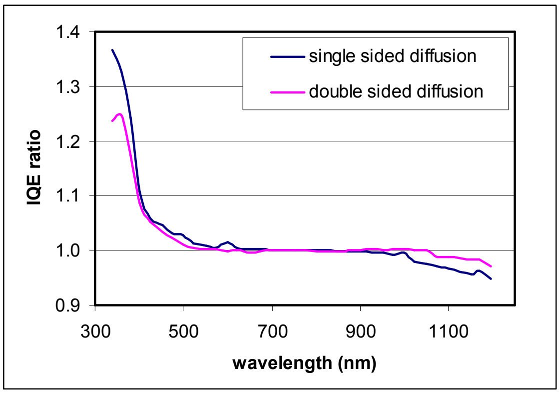

Figure 5: Internal Quantum Efficiency (IQE) ratio of the ECN-clean over the HF clean for both the single sided diffused group and the double sided diffused group.

3.3 PC1D modeling

In order to check the above stated conclusions PC-1D model calculations have been performed. First, a parameter set has been realized which gives a good fit to both the measured IQE and measured IV characteristics of an average cell in group 1 (single sided diffusion and no extra clean).

The influence of the double sided diffusion is gettering. This means that we expect an increase of the bulk lifetime of the cell. Therefore, in the second step only the bulk lifetime was increased to fit the IQE and IV data of group 3 (double sided diffusion, no clean).

Because the influence of the ECN-clean is in an increase of the blue response only, in the thirth step the front surface recombination velocity was decreased to fit the IQE and IV data of group 2 (single sided diffusion, ECN-clean).

Finally, in the fourth step the new τ_{bulk} and S_{front} as obtained in step 2 and 3 were used to calculated the IQE and IV data of group 4 (double sided diffusion and ECN-clean). Figure 7 and Table 5 show that the agreement between the calculated and measured data is good. This supports the result from Figure 2 that the observed gains are additional to one another.
The steps in the modeling are visualised in Figure 6.

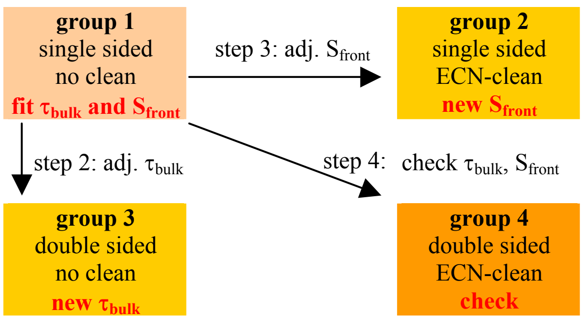

Figure 6: Steps used in the PC-1D modeling to check that the observed gains are additional to one another. In step 1, a parameter set is developed for group 1.

The input parameters for group 1 are given in Table 4. Figure 7 shows the IQE obtained for group 1 using these parameters. The modeled IV data together with the actual measured IV data are given in Table 5. Both the

IQE and the IV data are represented well by the parameter set.

Table 4: Input parameters PC-1D modeling group 1.

parameter	group 1
τ_{bulk}	12.5 µs
S_{rear}	750 cm/s
R_{rear}	70 %
S_{front}	$4{\cdot}10^6$ cm/s
R_{front}	experimental curve

[a]: This value is larger as compared to the values reported in our high efficiency papers because we had to use a different firing condition to obtain a good contact. In [9] we showed that S_{rear} is dependent on the firing conditions.

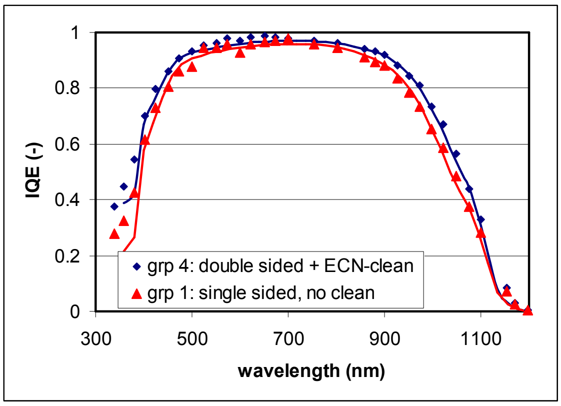

Figure 7: Measured IQE (points) and calculated IQE (solid lines) for group 1 and group 4.

Table 5: Results of PC-1D modeling. Data in red are from PC-1D modeling; data in black are experimental data. τ_{bulk} and S_{front} are the bulk lifetime and the front surface recombination velocity used in PC-1D

group	τ_{bulk} µs	S_{front} cm/s	J_{sc} mA/cm^2	V_{oc} mV	FF %	η %
1 exp.			31.6	595	76.9	14.5
PC-1D	12.5	$4{\cdot}10^6$	31.8	597	77.0	14.6
2 exp.			32.3	599	76.7	14.8
PC-1D	12.5	$1{\cdot}10^6$	32.3	600	76.9	14.9
3 exp.			32.4	602	76.4	14.9
PC-1D	25	$4{\cdot}10^6$	32.3	602	76.8	15.1
4 exp.			32.8	605	76.2	15.1
PC-1D	25	$1{\cdot}10^6$	33.0	605	76.8	15.4

3.4 Spin-on versus spray-on phosphorous source

Only recently the newly developed spray-on tool of Despatch became operational at ECN. Although the process was not yet fully optimized, homogeneous emitters have already been made (Figure 8).

A first direct comparison between spin-on and spray-on has been made by processing 2 sets of 20 neighboring wafers using ECN's baseline process sequence [10].

In Table 6 the obtained cell results are shown. With spray-on a small increase in both J_{sc} and V_{oc} is realized compared to spin-on, while the FF is slightly less. The average efficiency obtained for both groups are comparable. The large standard deviations result from the unintentional use of two different blocks of wafers within each group, one with a low material quality, the other with an average material quality. This has to be taken into account when the groups are compared [11], but in the standard deviation this is not done. The statistical analysis using this block effect reveals that the differences in J_{sc}, V_{oc}, FF and $J_{sc}{\cdot}V_{oc}$ are statistically significant at the 95% confidence level. The analysis thus shows that we have a statistically significant increase in both J_{sc} and V_{oc}. Due to a significant loss in FF of the same magnitude, the obtained efficiencies do not statistically differ.

Figure 9 shows the IQE-ratio of a spray-on cell over a spin-on cell. The increase in the blue response is small, and we have to do further investigations to fully understand the gain in J_{sc} and V_{oc} in using spray-on.

Also the difference in FF needs further examination. We used the baseline firing condition which is optimized for spin-on for both groups. It is not clear yet whether or not the spray-on emitter needs a different firing condition, or that the decrease in FF originates from the slightly larger inhomogeneity of the spray-on emitter.

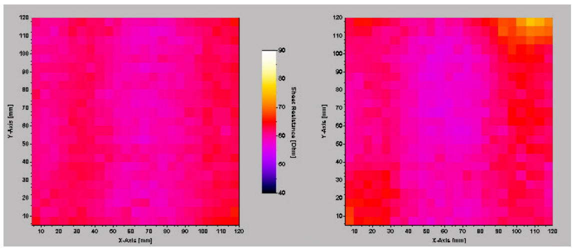

Figure 8: Sheet resistivity scans of spin-on (left) and spray-on (right) emitters. The vertical bands in the sheet resisitivity result from a known temperature inhomogeneity in the diffusion furnace. The sheet resisitivities of the 2 cells are comparable (respectively 58±2 Ω/sq for spin-on and 61±3 Ω/sq for spray-on).

Table 6: Average value solar cell characteristics; error margins given are the standard deviations.

group	J_{sc} mA/cm^2	V_{oc} mV	FF %	$J_{sc}\cdot V_{oc}$ mW/cm^2	η %
spin on	33.4±0.7	602±7	77.0±0.9	20.1±0.6	15.5±0.5
spray on	33.6±0.6	604±7	76.4±0.7	20.3±0.6	15.5±0.5

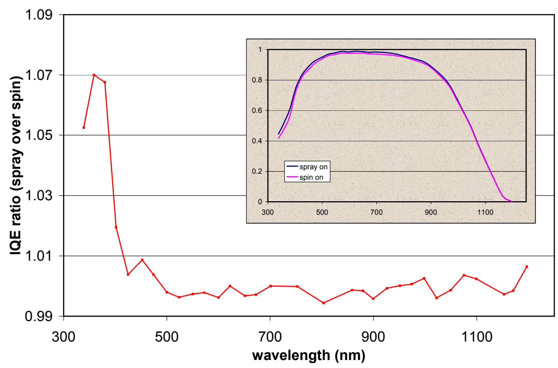

Figure 9: IQE ratio of spray-on over spin-on. Insert shows the IQE curves for both groups.

4 CONCLUSION

We presented 2 simple adjustments to an industrial processing sequence.

The first adjustment, applying the phosphorous source on both sides, increases the average efficiency by about 0.5% absolute. The efficiency increase is realized by an improved gettering which makes the processing less sensitive to the variation in material quality. Finally it drastically narrows the efficiency distribution.

The second adjustment, the ECN-clean after phosphorous glass removal, results in a better surface passivation. This gives an efficiency increase of about 0.3% absolute.

An absolute efficiency increase up to 1.3% has been observed. The average absolute efficiency increase is 0.8 %; 0.5% absolute efficiency increase is realized by increased gettering; 0.3% absolute efficiency increase is realized by better front surface passivation.

PC1D modeling supports the results of the experiment that the two effects are aditional effects.

Initial results with a new phosphorous srpay-on coater indicate that solar cells made with spray-on to apply the phosphorous source are at least comparable to solar cells made with spin-on coating.

ACKNOWLEDGEMENT

This work has been carried out with financial support of NovemSenter and performed within the Dutch DEN programme.

REFERENCES

[1] A.W. Weeber at al., Proceedings 20st European Photovoltaic Solar Energy Conference, Barcelona, (2005).
[2] C.J.J. Tool et al., Technical Digest 15th Int. Photovoltaic Science and Engineering Conference, Shanghai, (2005).
[3] C.J.J. Tool et al., Proceedings 31st IEEE Photovoltaic Specialist Conference, Florida, (2005).
[4] A.W. Weeber at al., this conference 2AO.2.2
[5] www.astm.com.
[6] www.statgraphics.com
[7] P.A. Basore, D.A. Clugston, PC-1D v5.5, University New South Wales 2000.
[8] M.J.A.A. Goris et al., Proceedings 29th IEEE Photovoltaic Specialist Conference, New Orleans, (2002).
[9] C.J.J. Tool et al., to be published in Sol. En. Mater. Sol. Cells. (2006).
[10] A.W. Weeber et al., this conference, presentation 2AO.2.3: 17% cell efficiency on large back-contacted multi-silicon solar cells.
[11] A.W. Weeber, W.C. Sinke, Proceedings 25th IEEE Photovoltaic Specialist Conference, p565 (1996).